Electronic Supplementary Information

Design of Hollow Spherical Co@hsZSM5@Metal Dual-Layer Nanocatalysts for Tandem CO_2 Hydrogenation to Increase C_{2+} Hydrocarbon Selectivity

Kelvin Mingyao Kwok[1,2], Luwei Chen[2,3]*, Hua Chun Zeng[1,]*

[1] *NUS Graduate School for Integrative Sciences and Engineering and Department of Chemical and Biomolecular Engineering, Faculty of Engineering, National University of Singapore, 10 Kent Ridge Crescent, Singapore 119260*

[2] *Department of Process & Catalysis Research, Institute of Chemical and Engineering Sciences, A*STAR (Agency for Science, Technology and Research), 1 Pesek Road, Jurong Island, Singapore 627833*

[3] *Department of Materials Science and Engineering, National University of Singapore, 9 Engineering Drive 1, Singapore 117576*

*Emails: chen_luwei@ices.a-star.edu.sg
chezhc@nus.edu.sg

Contents

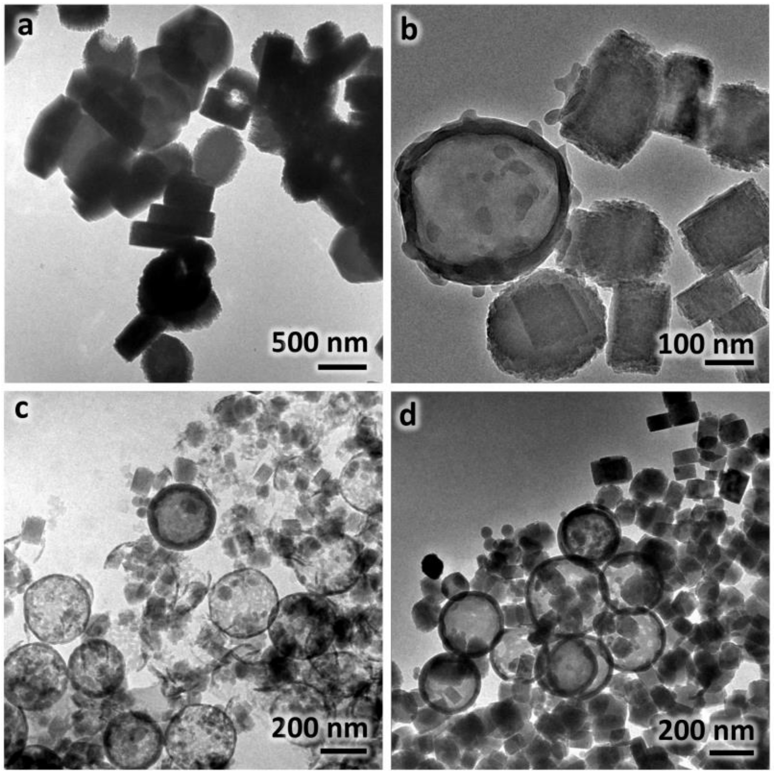

Figure S1. TEM images of morphology of attempted SiO_2 transformations to ZSM-5 at lower hydrothermal temperatures: (a) 155 °C, (b) 140 °C, (c) 125 °C, (d) 110 °C. Reducing hydrothermal treatment temperature does not result in hollow zeolite spheres, and a different approach of reducing the solution alkalinity and introducing PDDA is required.

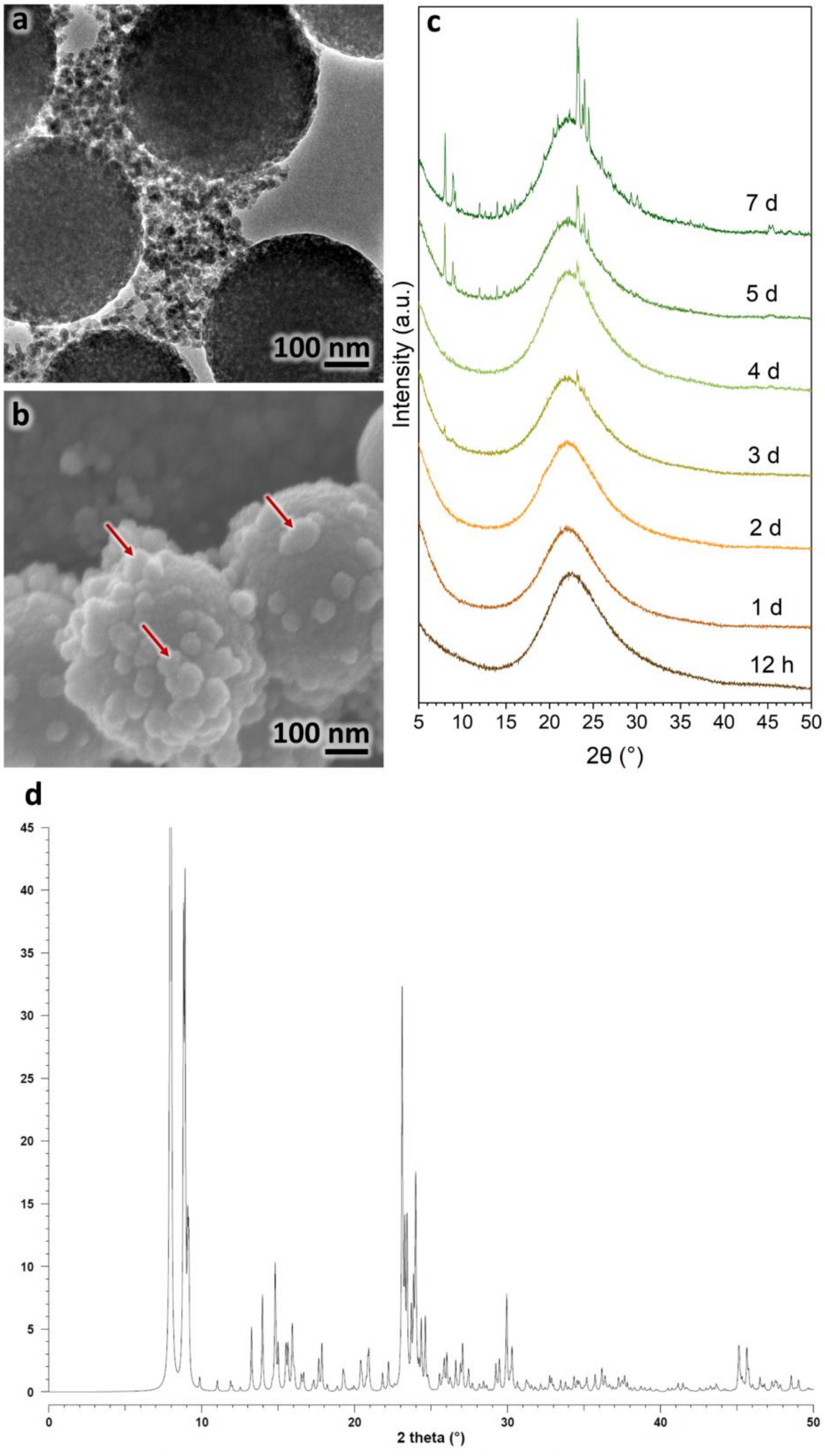

Figure S2. In-situ coating of ZSM-5 particles on the surface of solid SiO_2 sphere: (a) TEM image and (b) FESEM image of SiO_2@ZSM5 after 7 days of hydrothermal treatment; (c) XRD patterns from 12 h to 7 d of synthesis time; (d) simulated XRD pattern of ZSM-5, corresponding to JCPDS no. 89-1421. Reproduced with permission.[1]

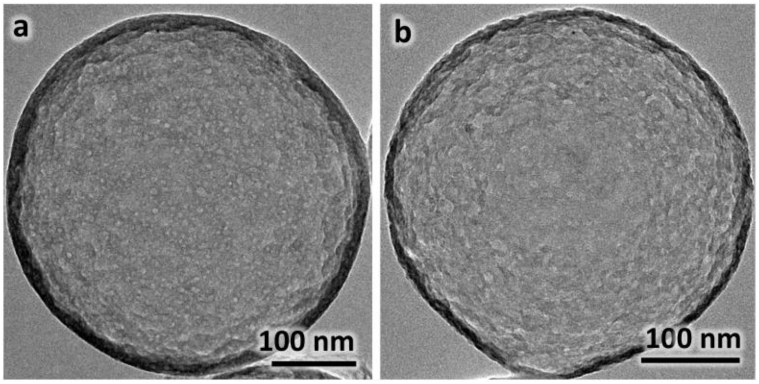

Figure S3. TEM images of hsZSM5 obtained after overnight etching with (a) 0.05 M NaOH and (b) 0.1 M NaOH. 50 mg of hsZSM5 was dissolved in 20 mL of NaOH solution for 16 h, and the resultant samples separated by centrifugation and washing with deionized water.

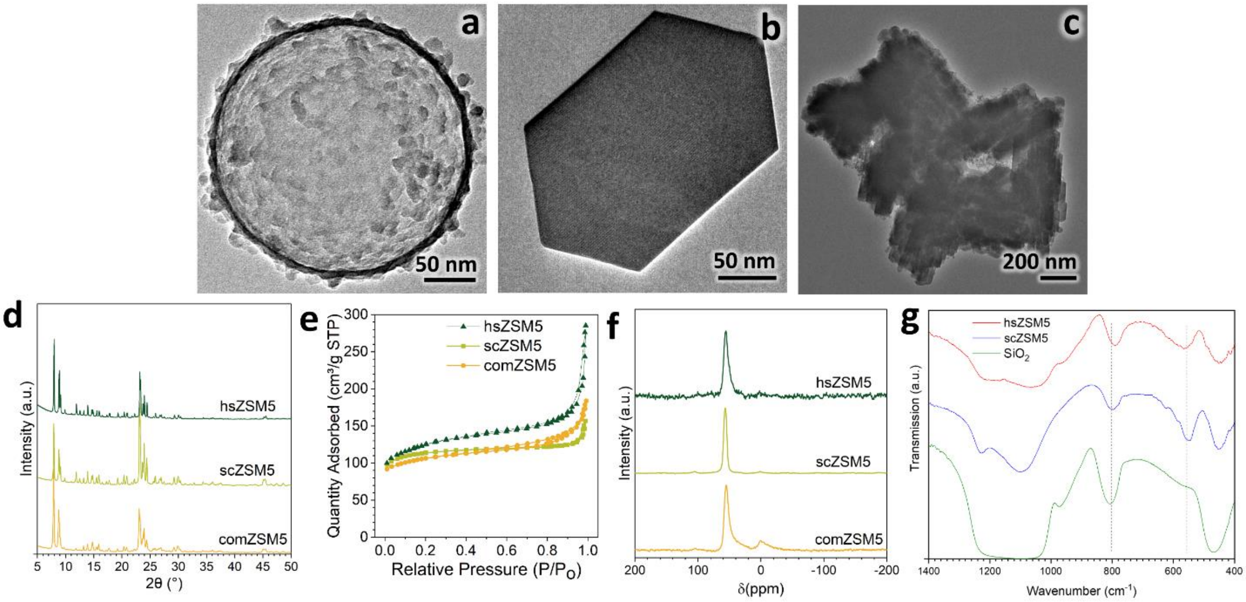

Figure S4. TEM images of (a) hsZSM5 and its corresponding Al distribution by EDS mapping, (b) scZSM5 and (c) comZSM5; (d) XRD patterns, (e) N_2 physisorption curves and (f) ^{27}Al solid-state NMR analysis of hsZSM5, scZSM5 and SiO_2.; (g) FTIR analysis of hsZSM5, scZSM5 and SiO_2. The presence of the IR band at 540-550 cm^{-1} for hsZSM5 and scZSM5 is a spectroscopic signature of the ZSM-5 (MFI framework) zeolite.[2]

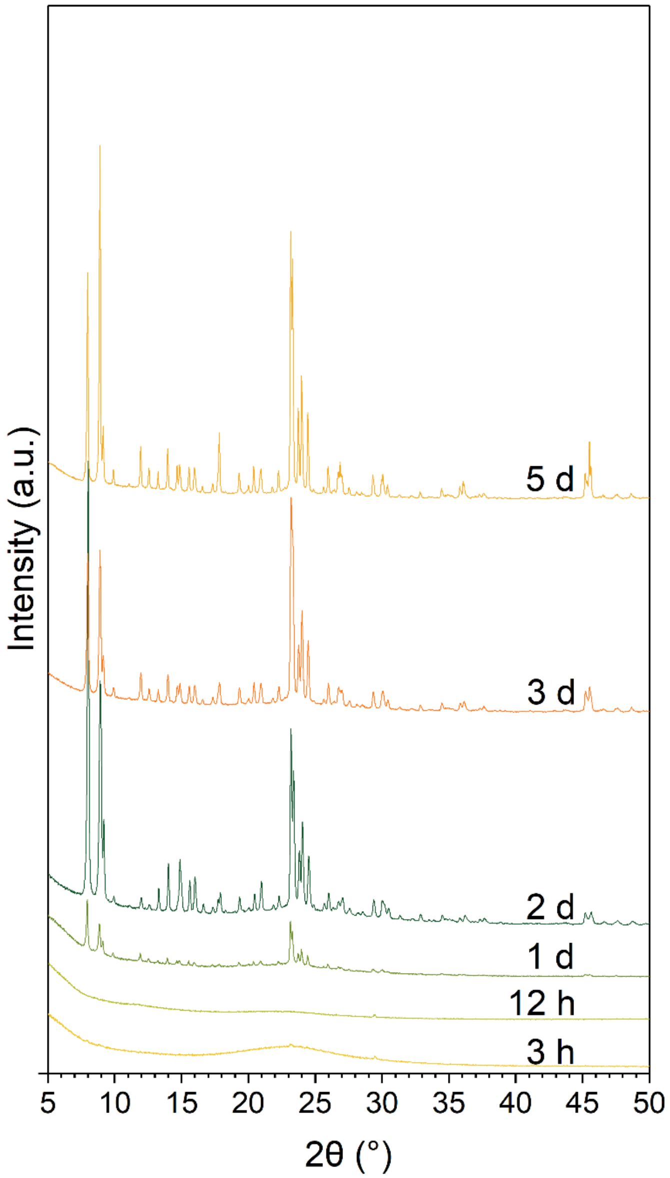

Figure S5. Time-dependent evolution of ZSM-5 zeolite shell observed via XRD characterization. The hsZSM5 sample is fully crystallized at 2 d. With increased synthesis time beyond 2 d, the XRD patterns do not change significantly.

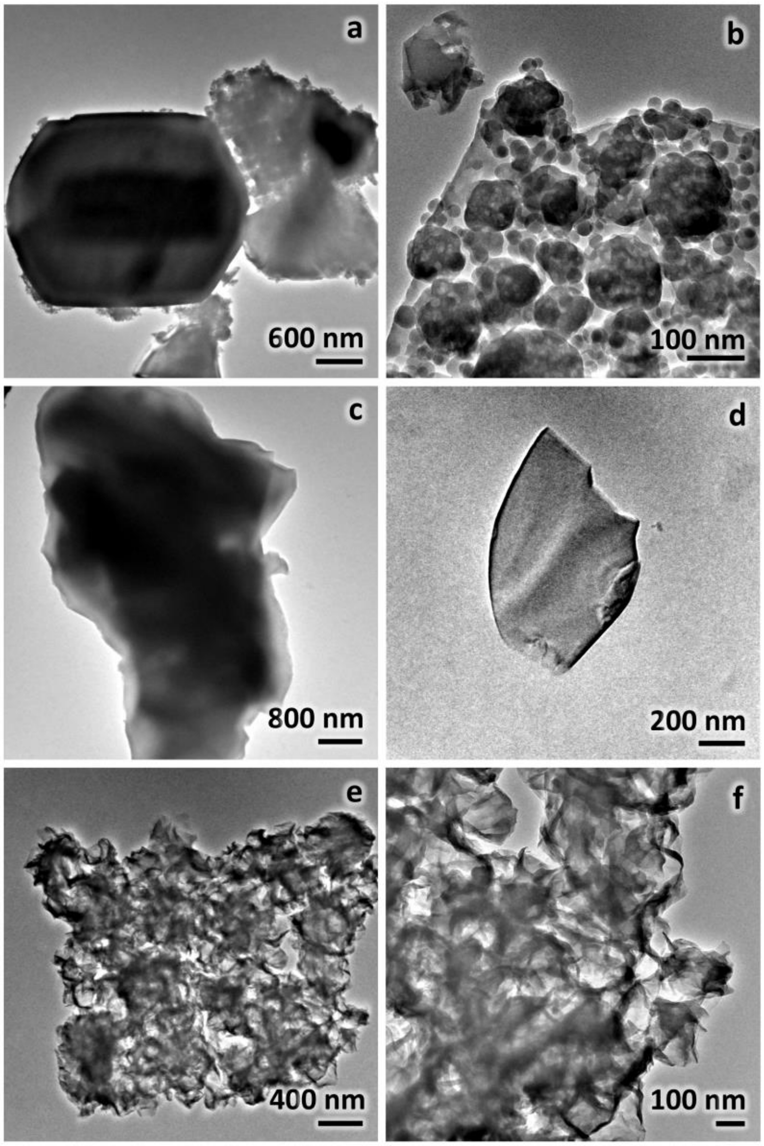

Figure S6. Using alternative surfactants for hsZSM5 synthesis results in suboptimal morphology. (a-b) TEM images of particles produced with polyvinylpyrrolidone (PVP) surfactant; (c-d) TEM images of particles produced with polyvinylalcohol (PVA) surfactant; (e-f) TEM images of particles produced with cetyltrimethylammonium bromide (CTAB) surfactant.

Synthesis conditions are similar to synthesis of hsZSM5 (Section 2.4 in main text) except that the 2 mL of aqueous 10 wt% poly(diallyldimethylammonium chloride) (PDDA) was replaced by aqueous 10 wt% of PVP / PVA / CTAB. This shows that only the positively charged PDDA is able to induce a hollow spherical zeolite morphology.

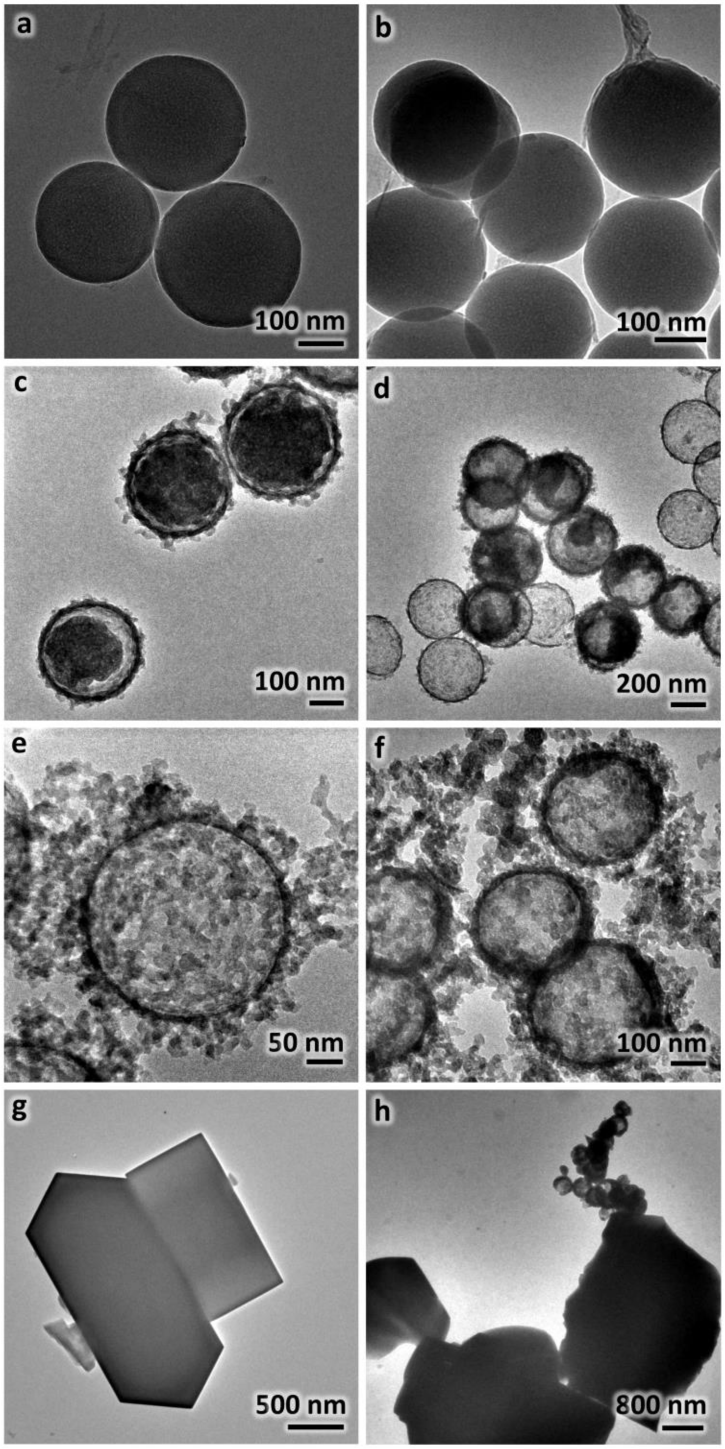

Figure S7. hsZSM5 synthesized with non-optimal parameters: TEM images of particles produced from synthesis mixture: (a) with no TPAOH or TPABr added, (b) with 10 mL of 1 M TPABr used instead of a mixture of 8 mL TPABr + 2 mL TPAOH, (c) with 311.7 mg of SiO_2 used instead of 211.8 mg, (d) with 0.5 wt% of PDDA used instead of 10 wt%, (e) with 158.9 mg of SiO_2 used instead of 211.8 mg, (f) with hydrothermal treatment at 150 °C instead of 170 °C, (g) with hydrothermal treatment at 200 °C instead of 170 °C, (h) with 6 mL TPABr + 4 mL TPAOH used instead of a mixture of 8 mL TPABr + 2 mL TPAOH. This shows that the synthesis of nanozeolite hollow sphere is sensitive to many synthesis parameters which must be optimized.

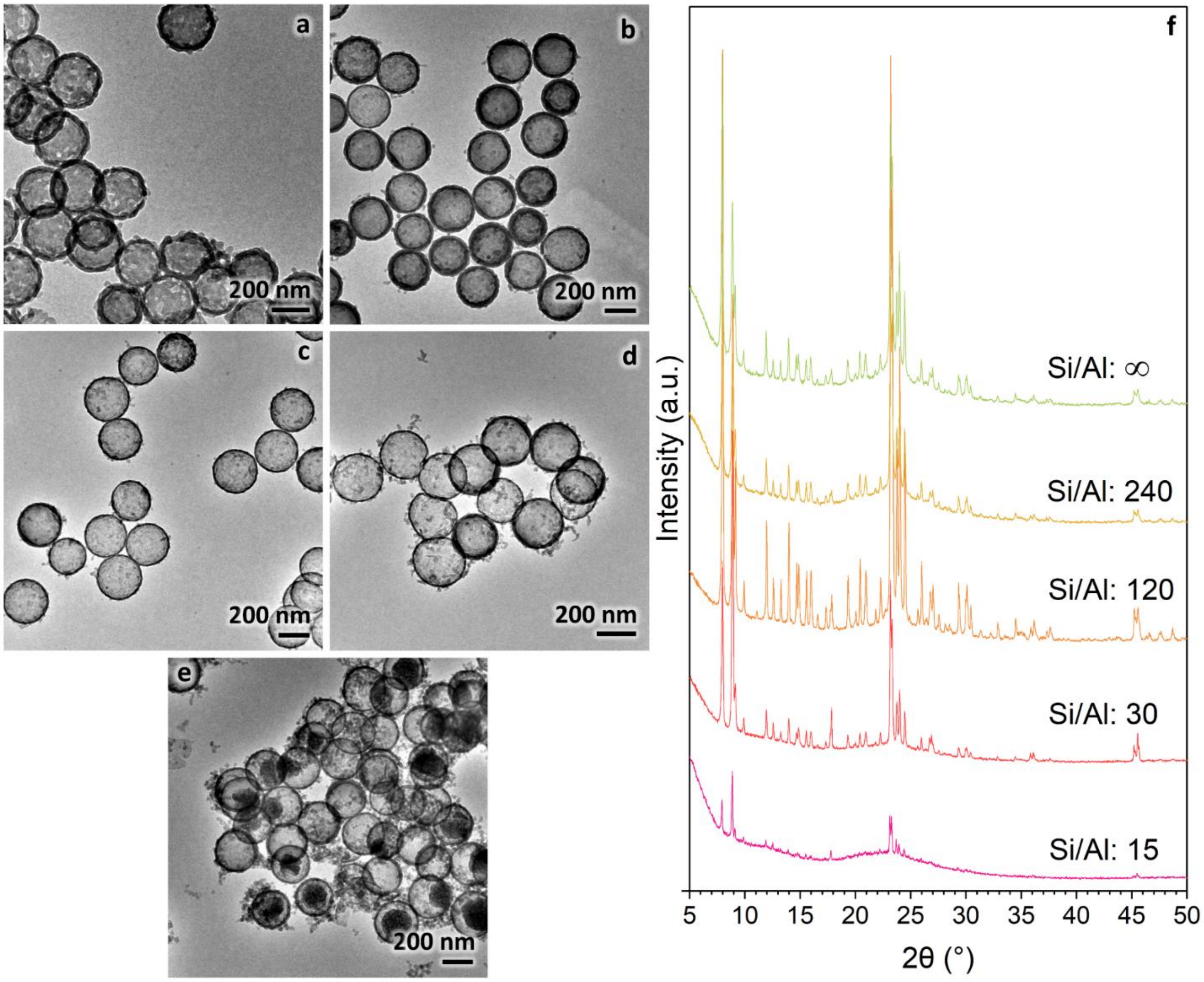

Figure S8. hsZSM5 synthesized with varying Si:Al ratio. TEM images of hsZSM5 synthesized with varying Si:Al ratios: (a) ∞, (b) 240, (c) 120, (d) 30, (e) 15. (f) corresponding XRD patterns of hsZSM5 with varying Si:Al ratios.

Synthesis of hsZSM5 was according to Methods except the amount of aluminum sulfate 18-hydrate added was decreased or increased accordingly (for Si:Al = 60, 19.6 mg of aluminum sulfate 18-hydrate was used). With Si:Al = 15, ZSM-5 is not fully crystallized, indicating a lower limit of about Si:Al = 30.

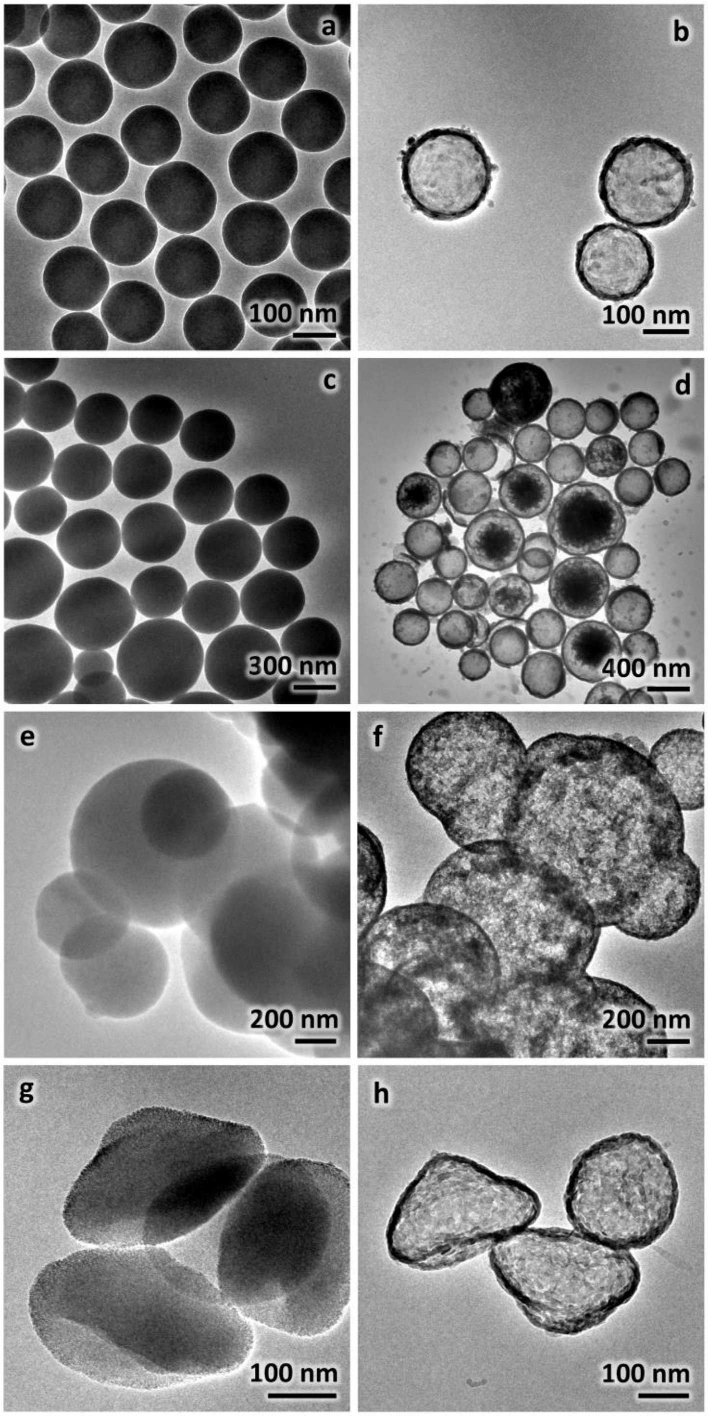

Figure S9. Morphology of hsZSM5 corresponds to initial SiO_2 particle shape. TEM images of different SiO_2 shapes and their corresponding hsZSM5 formed by the transformation to hsZSM5 (according to Methods): (a) smaller 100 nm SiO_2 spheres (synthesized with only 2.56 mL of 25% aqueous NH_3) and (b) corresponding smaller hsZSM5 sphere; (c) mixture of 200–600 nm SiO_2 spheres (synthesized with 24 mL TEOS and 10.24 mL NH_3) and (d) corresponding mixture of small and large hsZSM5 spheres; (e) merged mesoporous SiO_2 spheres (synthesized using 20 mL of ethanol) and (f) corresponding cloud-like hsZSM5 structures; (g) disc-shaped mesoporous SiO_2 (synthesized using 30 mg of ethanol-washed & dried Co_3O_4 nanocubes and 20mL of ethanol) and (h) corresponding disc-shaped hsZSM5 structures.

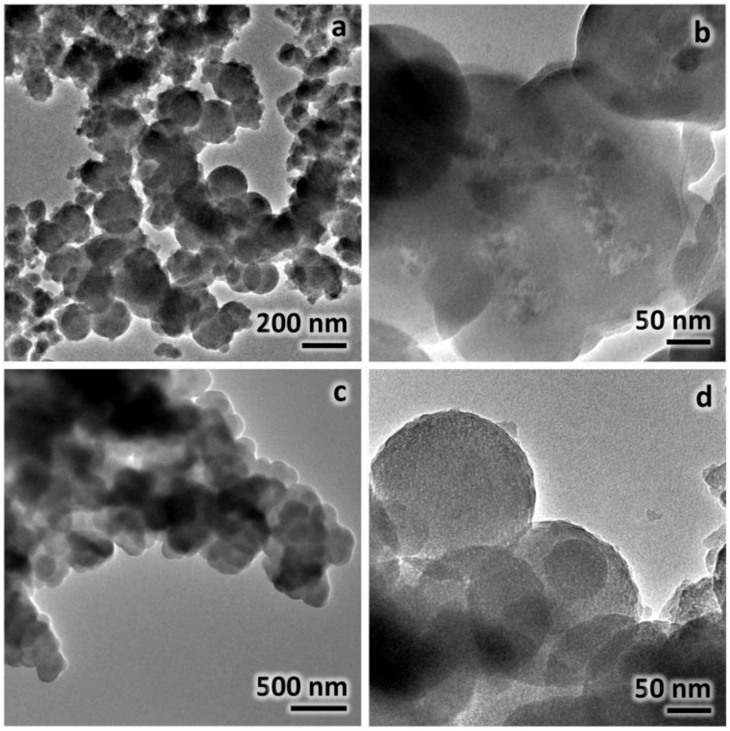

Figure S10. Morphology of SiO_2 spheres co-precipitated with transition metals. TEM images of (a) SiO_2 spheres doped with 10 wt% Co using $CoCl_2$, (b) the calcined product of (a). (c-d) TEM images of SiO_2 spheres doped with 10 wt% Ru using $RuCl_3$.

The products show that the metal ions interfere with the dispersion of the SiO_2 spheres resulting in merged-sphere morphology, while the calcined sphere in shows that Co_3O_4 can be observed as black particles in the core of the SiO_2.

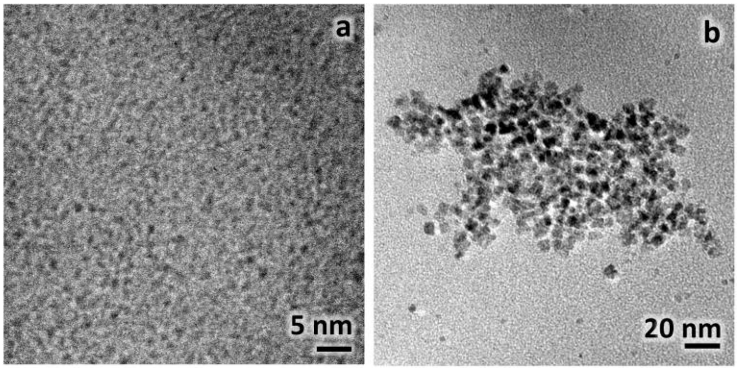

Figure S11. Metal nanoparticles synthesized ex-situ. (a) TEM images of Ru nanoparticles, (b) TEM images of Co_3O_4 nanoparticles.

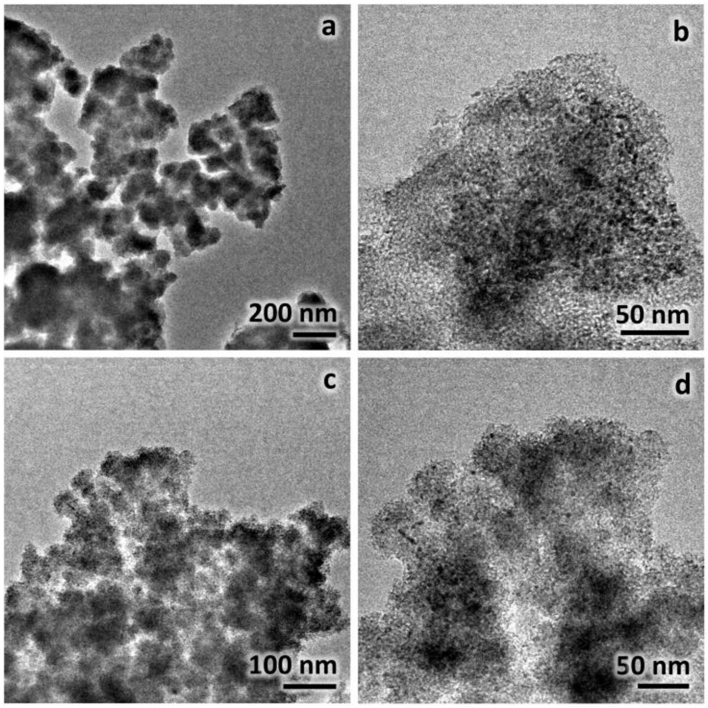

Figure S12. Co@SiO$_2$ synthesized with increased Co loading. (a-b) TEM images of Co@SiO$_2$ synthesized with 2 mL of Co$_3$O$_4$ nanocube solution, (c-d) TEM images of Co@SiO$_2$ synthesized with 4 mL of Co$_3$O$_4$ nanocube solution. The original Co@SiO$_2$ sample was synthesized with 1 mL of Co$_3$O$_4$ nanocube solution (Methods).

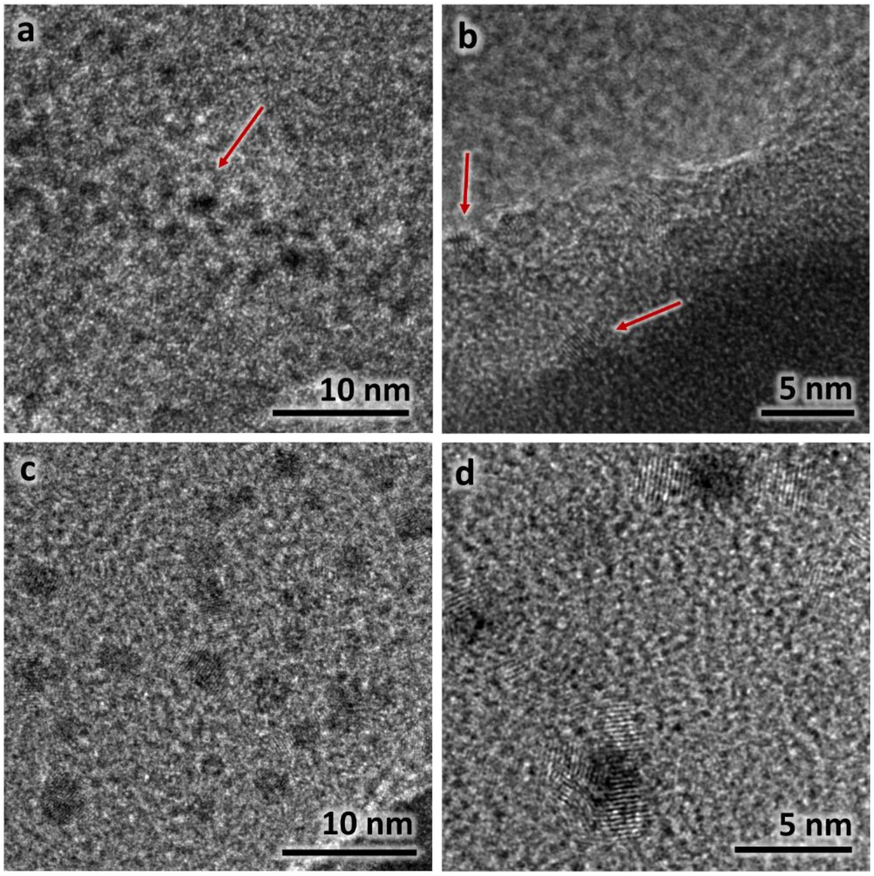

Figure S13. Noble metal nanoparticles deposited on hsZSM5. (a-b) high-resolution TEM images of hsZSM5@Ru with 1-2 nm Ru particle size. (c-d) high-resolution TEM images of hsZSM5@Pt with 2-5 nm Pt particle size.

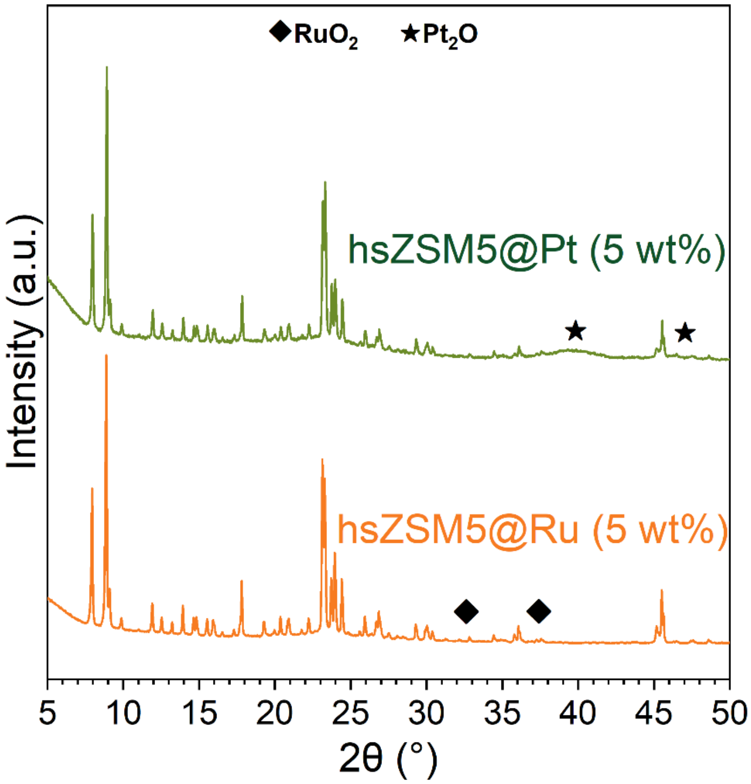

Figure S14. XRD patterns of hsZSM5@Pt (5 wt%) and hsZSM5@Ru (5 wt%). The broad peak at 39° for Pt_2O can be seen in hsZSM5@Pt (5 wt%) while no obvious peaks are seen for hsZSM5@Ru (5 wt%).

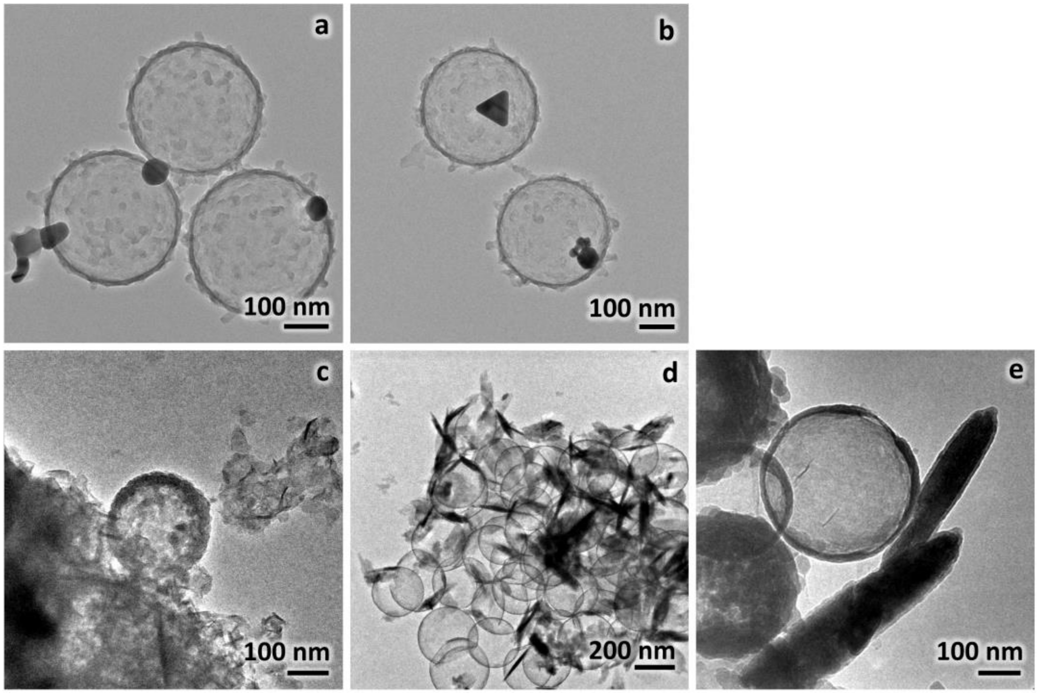

Figure S15. TEM images of hsZSM5 modified with unsuitable metals for the in-situ deposition method with 5 wt% loading. (a) Ag, (b) Au, (c) Co, (d) Cu, (e) Zn. Ag and Au form large particles due to the high hydrothermal temperature while Co, Cu and Zn form silicates due to the alkaline solution.

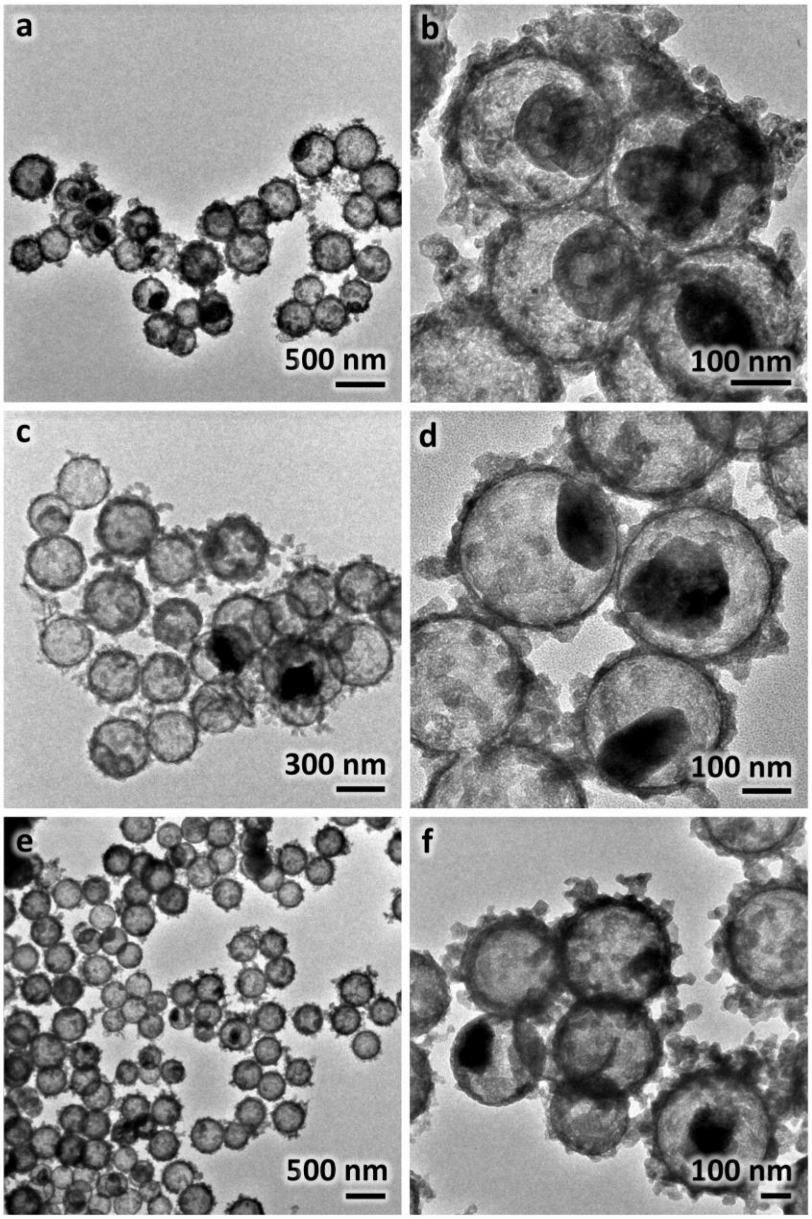

Figure S16. TEM images of hsZSM5 with metals added post-synthesis by incipient wetness impregnation: (a-b) Co, (c-d) Cu, (e-f) Zn.

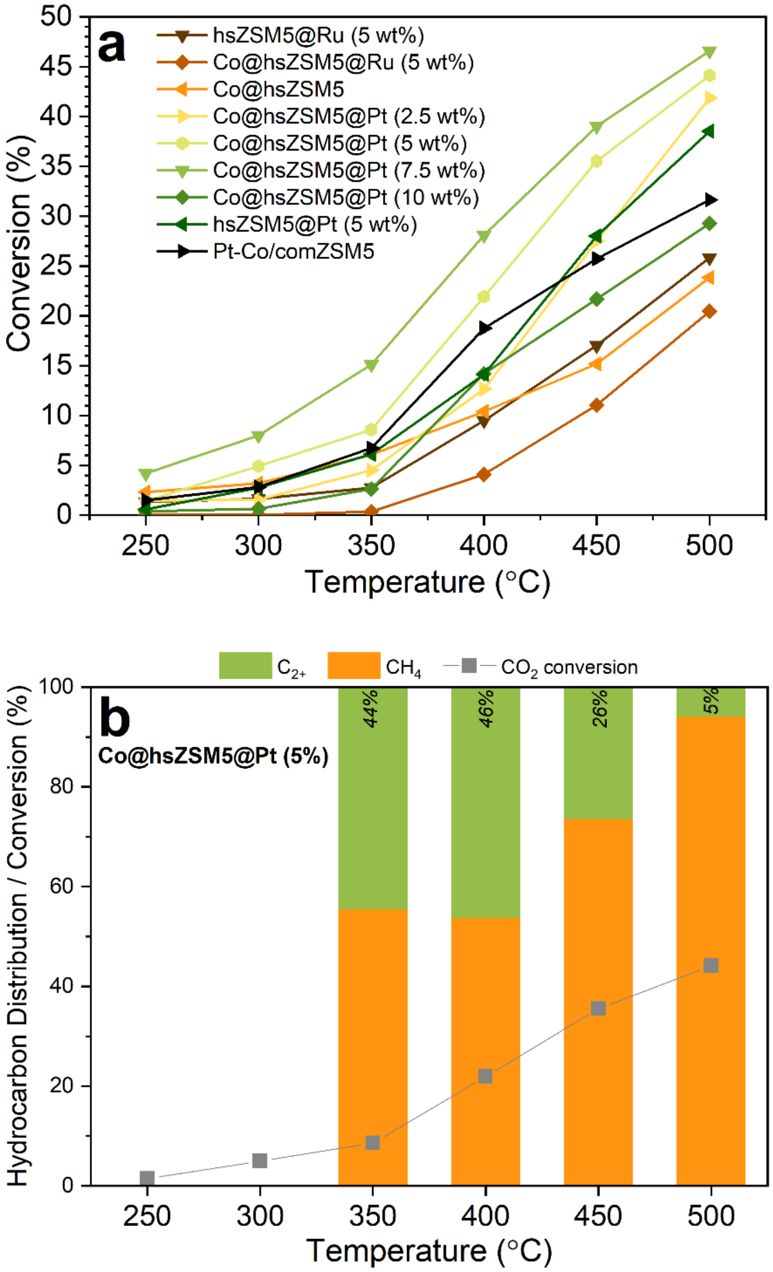

Figure S17. Catalytic performance at varying temperatures for CO_2 hydrogenation. (a) CO_2 conversion of various catalysts at different temperatures; (b) hydrocarbon distribution and CO_2 conversion of Co@hsZSM5@Pt (5 wt%). Reaction conditions: 200 mg catalyst, 15 mL/min of reaction gas (72 H_2 : 24 CO_2 : 4 N_2) at 20 bar. The percentages for Co@hsZSM5@Pt refer to weight loading of Pt. At 250-300°C, no hydrocarbons were produced (i.e. only CO was produced).

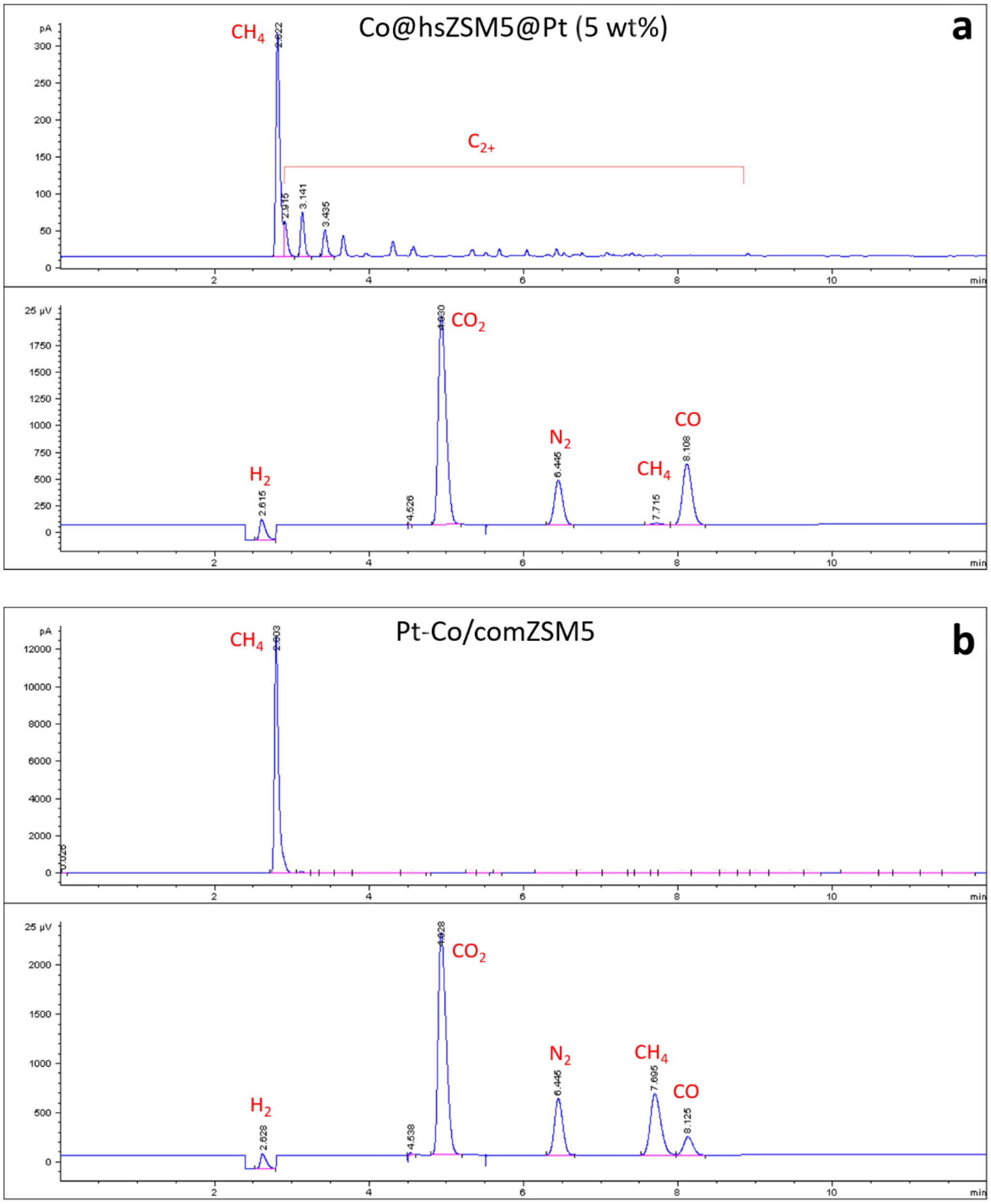

Figure S18. Gas chromatograms of the products of CO_2 hydrogenation. (a) Co@hsZSM5@Pt(5%) catalyst, (b) Pt-Co/comZSM5 catalyst.

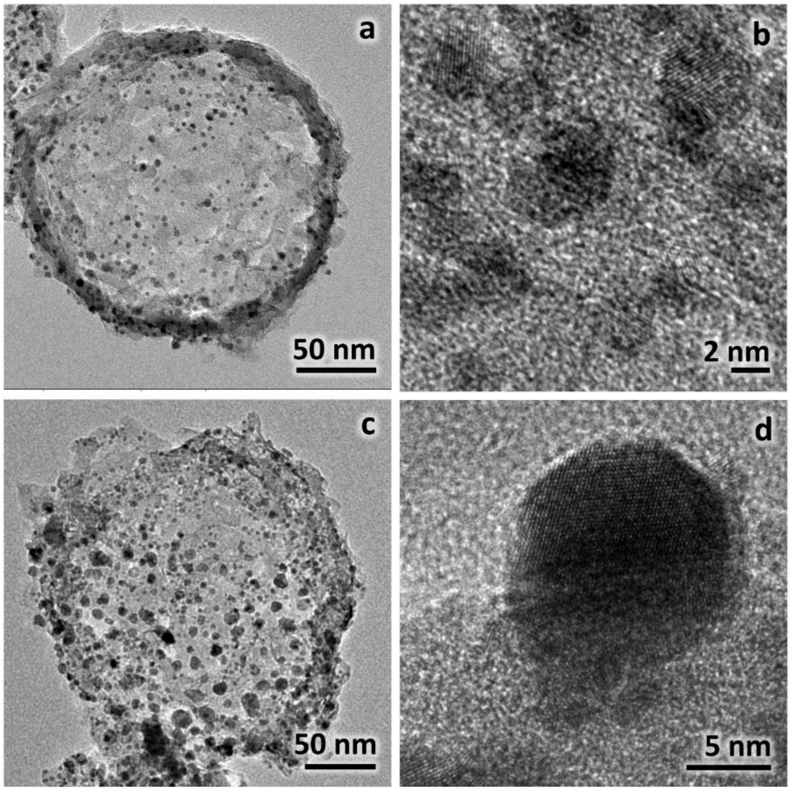

Figure S19. Morphology of spent catalysts after CO_2 hydrogenation: TEM images of (a-b), Co@hsZSM5@Pt (5 wt%), (c-d) Co@hsZSM5@Pt (10 wt%), Higher loading of 10 wt% Pt in Co@hsZSM5@Pt results in larger crystallite sizes than 5 wt%; PtCo alloy can be seen in the EDX scans of Pt-Co/comZSM5 (h).

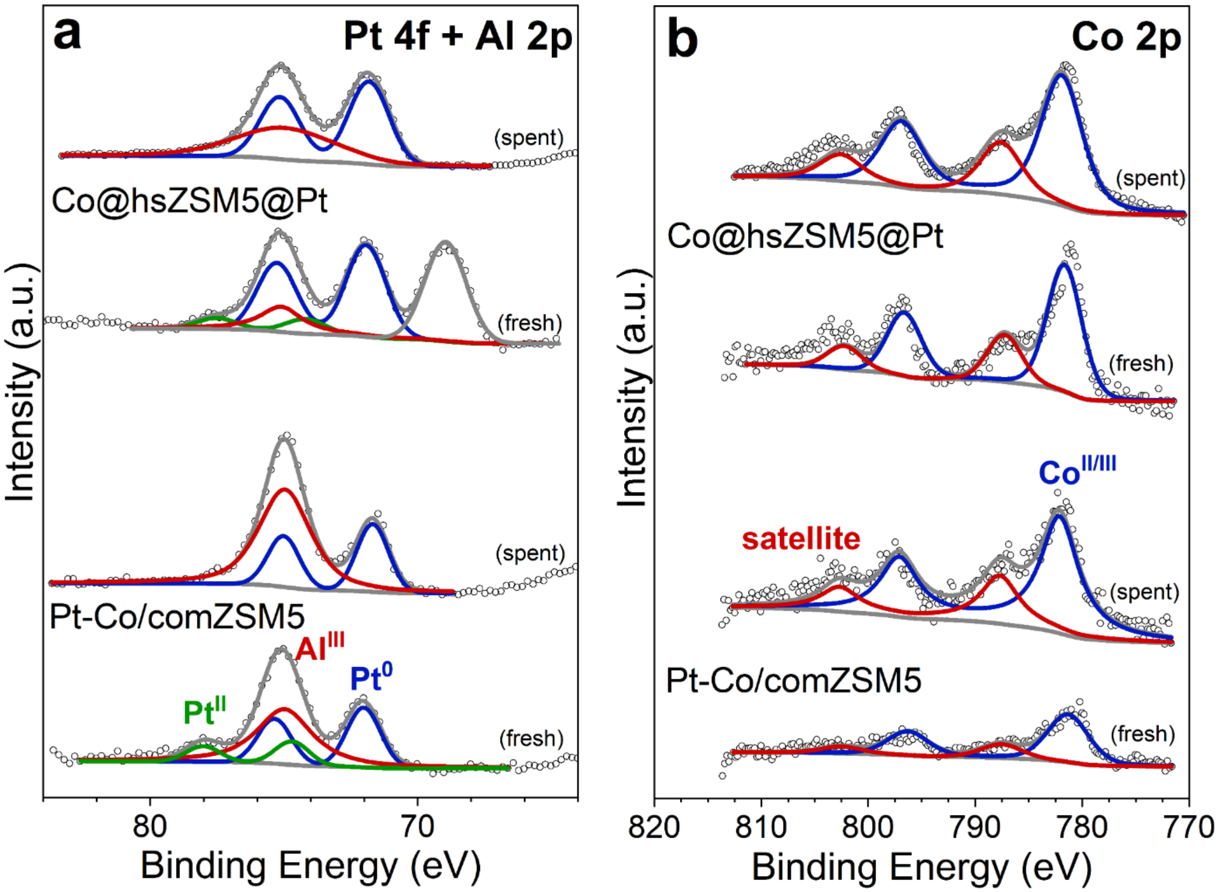

Figure S20. XPS spectra of fresh and spent Co@hsZSM5@Pt (5 wt%) and Pt-Co/comZSM5 catalysts: (a) Pt 4f + Al 2p spectra, (b) Co 2p spectra. The Al 2p signal overlaps with Pt 4f.

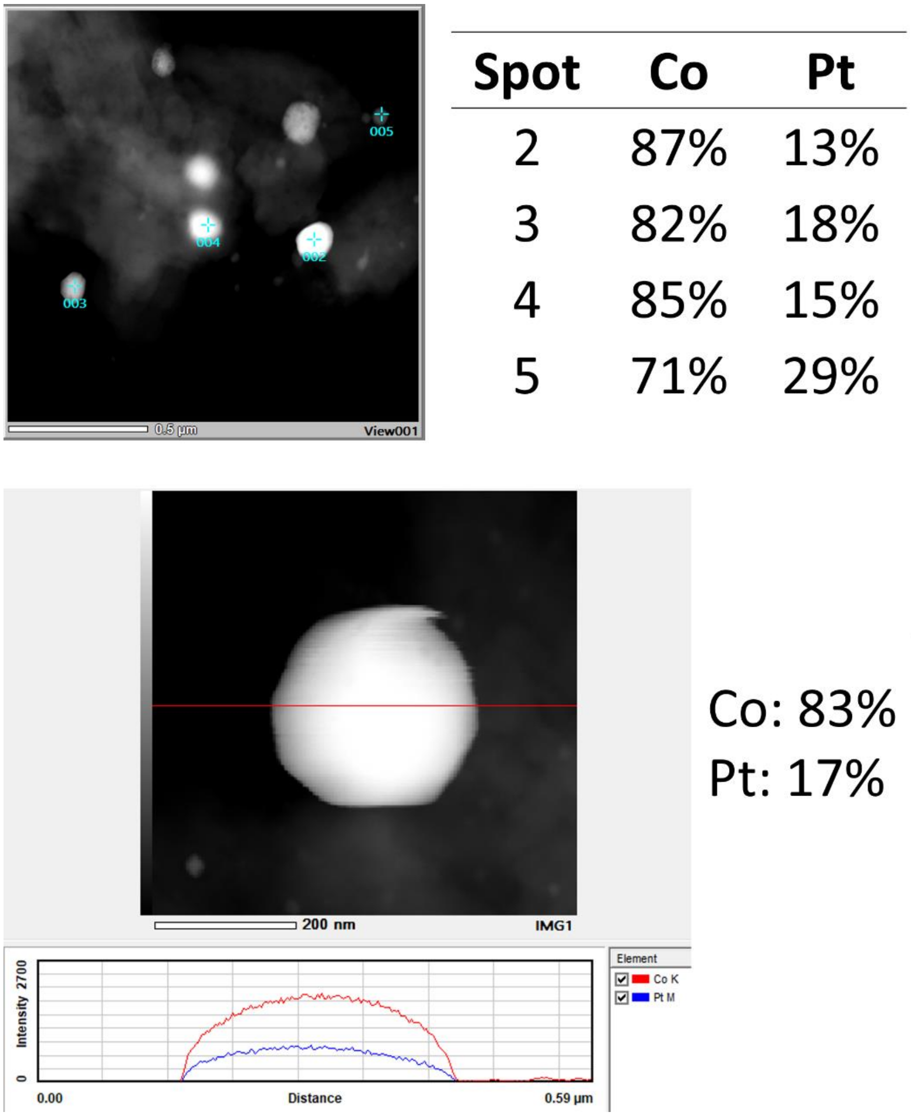

Spot	Co	Pt
2	87%	13%
3	82%	18%
4	85%	15%
5	71%	29%

Co: 83%
Pt: 17%

Figure S21. EDS spot scan and line scans of spent Pt-Co/comZSM5 catalyst. Spot scans are indicated by the cyan cross marks in the TEM image and the line scan across one particle is indicated by the red line.

Table S1. Summary of metal composition in metal-doped hsZSM5 and conventional catalysts measured from XRF.

Sample	Metal content (wt%)
hsZSM5@Ru (5 wt%)	4.4% Ru
Co@hsZSM5@Ru (5 wt%)	8.1% Co, 4.3% Ru
Co@hsZSM5	8.3% Co
Co@hsZSM5@Pt (5 wt%)	7.7% Co, 5.6% Pt
hsZSM5@Pt (5 wt%)	5.8% Pt
Pt-Co/comZSM5	8.2% Co, 5.2% Pt

Table S2. Catalytic performance of hsZSM5-supported layered Ru/Co/Pt nanocatalysts for CO_2 hydrogenation. Reaction conditions: 200 mg of catalyst, 400 °C, 15 $mL \cdot min^{-1}$ of reaction gas (72 H_2 : 24 CO_2 : 4 N_2) at 20 bar. Loading of Co is constant at 8 wt%, while loading of outer metal layer is indicated. Pt-Co/comZSM5 has the same metal loading as Co@hsZSM5@Pt (5 wt%). Note that the hydrocarbon selectivity is only among all hydrocarbons (i.e. excludes CO).

Catalyst	CO_2 conversion	CH_4 hydrocarbon selectivity	C_{2+} hydrocarbon selectivity	CO selectivity
hsZSM5@Ru (5 wt%)	9.5%	99.3%	0.7%	18.7%
Co@hsZSM5@Ru (5 wt%)	4.1%	73.6%	26.4%	64.1%
Co@hsZSM5	10.4%	100%	0%	34.5%
Co@hsZSM5@Pt (2.5 wt%)	12.7%	76.9%	23.1%	58.8%
Co@hsZSM5@Pt (5 wt%)	21.9%	53.8%	46.2%	58.4%
Co@hsZSM5@Pt (7.5 wt%)	28.1%	59.8%	40.2%	61.5%
Co@hsZSM5@Pt (10 wt%)	14.2%	87.8%	12.2%	56.5%
hsZSM5@Pt (5 wt%)	14.1%	99.8%	0.3%	49.5%
Pt-Co/comZSM5	18.8%	98.9%	1.1%	10.5%

References

1. M.M.J. Treacy, J.B.Higgins, Collection of Simulated XRD Powder Patterns for Zeolites, 5th Edition (2001)

2. Lesthaeghe, D., Vansteenkiste, P., Verstraelen, T., Ghysels, A., Kirschhock, C. E. A., Martens, J. A., Speybroeck, V. V., Waroquier, M. MFI Fingerprint: How Pentasil-Induced IR Bands Shift during Zeolite Nanogrowth. *J. Phys. Chem. C* **2008**, 112, 25, 9186-9191.